

## Publication information

Title	Do droplets always move following the wettability gradient?
Author(s)	Wu, Jun; Ma, Ruiyuan; Wang, Zuankai; Yao, Shuhuai
Source	Applied physics letters , v. 98, (20), May 2011, article number 204104
Version	Published version
DOI	<a href="http://dx.doi.org/10.1063/1.3592997">http://dx.doi.org/10.1063/1.3592997</a>
Publisher	American Institute of Physics (AIP) Publishing

## Copyright information

This article may be downloaded for personal use only. Any other use requires prior permission of the author and AIP Publishing. The following article appeared in "Wu, J., Ma, R., Wang, Z., Yao, S. (2011). Do droplets always move following the wettability gradient? Applied physics letters, 98(20), article number 204104." and may be found at <http://dx.doi.org/10.1063/1.3592997>

## Notice

This version is available at HKUST Institutional Repository via <http://hdl.handle.net/1783.1/34875>

If it is the author's pre-published version, changes introduced as a result of publishing processes such as copy-editing and formatting may not be reflected in this document. For a definitive version of this work, please refer to the published version.



## Do droplets always move following the wettability gradient?

Jun Wu, Ruiyuan Ma, Zuankai Wang, and Shuhuai Yao

Citation: *Applied Physics Letters* **98**, 204104 (2011); doi: 10.1063/1.3592997

View online: <http://dx.doi.org/10.1063/1.3592997>

View Table of Contents: <http://scitation.aip.org/content/aip/journal/apl/98/20?ver=pdfcov>

Published by the AIP Publishing

---

### Articles you may be interested in

[Automatic droplet transportation on a plastic microfluidic device having wettability gradient surface](#)

*Rev. Sci. Instrum.* **86**, 015001 (2015); 10.1063/1.4905530

[Wettability model for various-sized droplets on solid surfaces](#)

*Phys. Fluids* **26**, 082110 (2014); 10.1063/1.4893935

[Freezing of sessile water droplets on surfaces with various roughness and wettability](#)

*Appl. Phys. Lett.* **104**, 161609 (2014); 10.1063/1.4873345

[Lattice Boltzmann study of droplet motion inside a grooved channel](#)

*Phys. Fluids* **21**, 022103 (2009); 10.1063/1.3077800

[Asymptotic theory for a moving droplet driven by a wettability gradient](#)

*Phys. Fluids* **18**, 042104 (2006); 10.1063/1.2191015

---

A promotional banner for an Agilent Technologies webinar. The background shows a scientist in a lab coat working with a complex piece of equipment. The text 'WHAT YOU NEED TO KNOW ABOUT VACUUM' is in yellow and white. Below it, a pink box contains 'WEBINAR SERIES' and a blue box contains 'SIGN UP TODAY'. The Agilent Technologies logo and name are at the bottom.

**WHAT YOU NEED  
TO KNOW ABOUT VACUUM**

**WEBINAR SERIES**

**SIGN UP TODAY**

Agilent Technologies

## Do droplets always move following the wettability gradient?

Jun Wu,<sup>1</sup> Ruiyuan Ma,<sup>1</sup> Zuankai Wang,<sup>2,a)</sup> and Shuhuai Yao<sup>1,a)</sup>

<sup>1</sup>Department of Mechanical Engineering, The Hong Kong University of Science and Technology, Kowloon, Hong Kong

<sup>2</sup>Department of Manufacturing Engineering and Engineering Management, City University of Hong Kong, Kowloon, Hong Kong

(Received 7 April 2011; accepted 26 April 2011; published online 19 May 2011; publisher error corrected 25 May 2011)

Impacting droplets on rough surfaces with a wettability gradient have been reported to rebound obliquely or migrate following the wettability gradient due to the unbalanced interfacial forces created by such heterogeneous architectures. Here we demonstrate under certain conditions, droplets can be self-propelled against the wettability gradient. We show that the local Cassie-to-Wenzel transition in the droplet is critical for such a counter-intuitive phenomenon. We believe that our letter extends our conventional understanding of wettability dynamics to heterogeneous surfaces and provides important insight for the design of micro/nanotextured surfaces for controlled droplet manipulation. © 2011 American Institute of Physics. [doi:10.1063/1.3592997]

Droplet impact on surfaces, a complex dynamic phenomenon that occurs on the three-phase interface, plays an important role for a variety of technical applications including ink-jet printing, spray coating, spray cooling, solder deposition, and anti-icing.<sup>1</sup> Previously, it has been shown that droplets impacting on superhydrophobic surfaces with uniform structures exhibit various patterns from complete rebounding to sticking, and the spreading and receding processes of droplets remain symmetrical.<sup>1–8</sup> Surfaces with large energy barrier between the Cassie and Wenzel states ( $E_{c-w}$ ) to withstand a high impact velocity are energetically favored for elastic rebounding.<sup>8</sup>

Different from the symmetrical response on the uniform textured surfaces, the droplets impacting on heterogeneous surfaces may exhibit more complicate dynamic patterns. Our previous work and others have shown that impacting droplets on surfaces with roughness (wetting) gradient rebound obliquely<sup>9,10</sup> or migrate<sup>11</sup> spontaneously following the direction of wettability [i.e., toward the direction of smaller static contact angle (CA)] due to the existence of lateral force caused by wetting difference across the droplets. However, in these letters, the droplets on such nonuniform surfaces maintain in the Cassie state where the impacting energy is smaller compared to the  $E_{c-w}$ . Because the energy barrier of the Cassie-to-Wenzel transition ( $E_{c-w}$ ) is governed by the surface morphology and the intrinsic CA,<sup>8</sup> for a nonuniform textured surface (e.g., with a controlled wettability gradient),  $E_{c-w}$  should vary in space. Thus, under the same impacting condition, we hypothesize that the global droplet response upon impact on a nonuniform textured surface will be significantly influenced by the local wetting dynamics, and thereby fashion strikingly different patterns from the previously reported results. In this letter we explore the droplet impact dynamics on a superhydrophobic surface with a roughness gradient under various impacting conditions. Counter-intuitively, we found that under some conditions, the droplet did not move following the direction of decreasing static CA, instead, it

moved against the direction of the wettability gradient.

A nonuniform texture was created via microfabrication by patterning a surface with varying center-to-center spacing between micropillars<sup>12,13</sup> from 70  $\mu\text{m}$  in the sparsest region to 10  $\mu\text{m}$  in the densest region, over a span of 3.5 mm. The micropillar diameter  $a$  and height  $h$  are 10  $\mu\text{m}$  and 20  $\mu\text{m}$ , respectively. The etched substrate was treated by  $\text{CH}_4$  to form a uniform fluorocarbon layer with intrinsic static CA of  $\sim 101^\circ$ . The scanning electron microscopy (SEM) image of the as-fabricated surface is shown in Fig. 1. To characterize the static and dynamic wetting properties of each section, we also fabricated seven individual samples with uniform pillar spacing  $b$  (varied from 10 to 70  $\mu\text{m}$ ). The static CA, receding CA, and advancing CA of these individual samples all increase as the solid fraction  $f = (\pi a^2)/(4b^2)$  decreases,<sup>14</sup> which is consistent with the Cassie's law<sup>15</sup> and the experimental results reported by Yeh *et al.*<sup>16</sup> and Dorrer and Ruhe.<sup>17</sup> The local, static CA gradient for our gradient surface was found to be  $\sim 13^\circ/\text{mm}$ .

We performed the impact experiments on the nonuniform textured surface. A 4.2  $\mu\text{L}$  de-ionized water droplet of

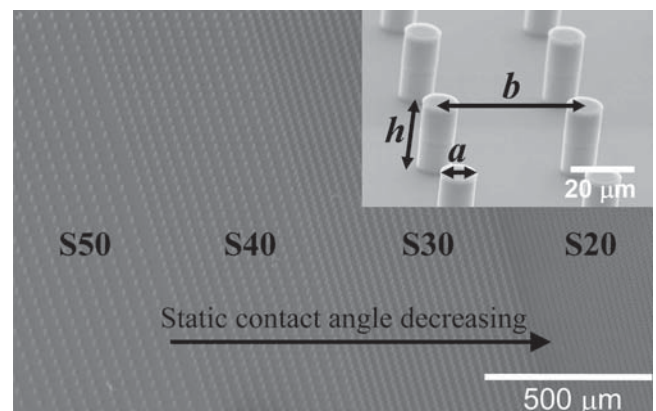


FIG. 1. Angle-view SEM image of the gradient surface with nonuniform surface roughness. The dimensions of the micropillar patterns are indicated as in the inset: the diameter  $a=10 \mu\text{m}$ , the height  $h=20 \mu\text{m}$ , and the center-to-center spacing  $b$  varies from 10 to 70  $\mu\text{m}$ , resulting in static CA of water from  $123^\circ$  to  $169^\circ$ . The micropillar sections are noted as 'Sb' (i.e., S10 to S70).

<sup>a)</sup>Authors to whom correspondence should be addressed. Electronic addresses: zuanwang@cityu.edu.hk and meshyao@ust.hk.

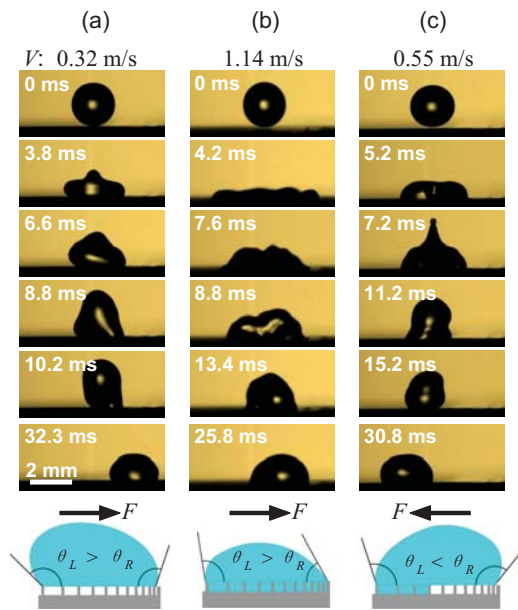


FIG. 2. (Color online) Snapshots of a  $4.2 \mu\text{L}$  water droplet impacting on the gradient surface at different impact velocities: (a)  $V=0.32 \text{ m/s}$ , (b)  $V=1.14 \text{ m/s}$ , and (c)  $V=0.55 \text{ m/s}$ . In all cases, the droplets do not rebound completely from the surface but are directed in lateral displacements due to the dynamic response of wetting on the gradient surface associated with different impact velocities. The schematics at the bottom show the droplets in contact with the micropillars before receding at different impact velocities, in which  $\theta_L$  and  $\theta_R$  are the receding CAs on both sides. The arrow shows the direction of unbalanced Young's force.

diameter 2 mm water was released from a height of 5.1 mm (corresponding to an impact velocity of 0.32 m/s) impacting on the gradient surface centered at the junction of S30 and S40. The impact process was recorded by a high speed camera (HG-100k, Redlake) at 5000 fps. In the spreading process, it was found that the spread droplet exhibited an asymmetric shape as shown at 3.8 ms in Fig. 2(a). Careful observation of local CA also found that the advancing CA on the left front of droplet (at the boundary of S50 and S60) was much larger than that on the right front (at the boundary of S10 and S20). During the receding process, the receding CA on the left was also higher than that on the right, and the receding CAs on both sides were higher than  $130^\circ$ . Such higher local receding CAs suggest that the droplet stays in the Cassie state. Under nonsticking Cassie state, the solid-liquid adhesion force is small and the droplet is easily influenced by the lateral force at the solid-liquid interfaces. The Young's force on the opposite sides of liquid-solid contact line can be expressed as:  $dF = \gamma(\cos \theta_1 - \cos \theta_2)ds$ , where  $F$  is the Young's force,  $\gamma$  is the surface tension of water,  $\theta_1$  and  $\theta_2$  are the receding CAs on both sides, and  $s$  is the length of contact line.<sup>18</sup> It is obvious that under such a driving force, the droplet is vectored in the direction of decreasing CA.

Figure 2(b) shows the snapshots of droplet impacting on the same surface at a much higher impacting velocity 1.14 m/s. We found that the droplet also migrated toward the direction of decreasing CA, although the migration was not apparent as that at lower impacting velocity. The large impact velocity caused the water penetrated into the micropillars and the entire droplet was in the Wenzel state, indicated by relatively small receding CAs ( $<90^\circ$ ) of both sides [the snapshot of Fig. 2(b) at 7.6 ms]. Once in the Wenzel state, a smaller receding CA is generated because of larger rough-

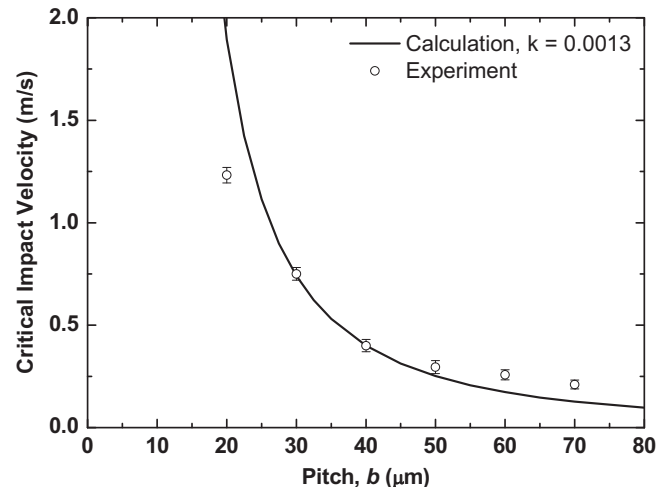


FIG. 3. The critical impact velocities at which a droplet can completely rebound for various uniform textured surfaces. Shown together are the experimental data (open circles) and a theoretical curve by considering the competition between the water hammer pressure and capillary pressure. The region above the curve represents the Wenzel state and below is the Cassie state of the droplet upon collision.

ness on the right side,<sup>16,19</sup> indicated in the snapshots of Fig. 2(b) from 7.6 to 13.4 ms ( $\theta_L > \theta_R$ ). As the droplet remained pinned on the surface, it drifted slightly from left to right under the unbalanced Young's force.

Interestingly, when the impact velocity was set between the above two cases (e.g.,  $V=0.55 \text{ m/s}$ ), we found the droplet did not follow the direction of decreasing CA (wettability gradient), but shifted toward the area wetted by the impacting pressure. As shown in Fig. 2(c), the left CA appeared smaller than the right one upon impact. During the retraction stage, the receding CA on the left was consistently smaller than that on the right ( $\theta_L < \theta_R$ ), thus created a lateral displacement to the left, which, unexpectedly, was opposite to the direction of the wettability gradient. Consistent result of droplet displacement was shown by reversing the orientation of the surface. Careful observation revealed that the receding CA on the left was less than  $90^\circ$  while as the receding CA on the right was more than  $130^\circ$ , suggesting that the left part of droplet might transition to sticky Wenzel state during impact.

The strikingly different impact dynamics might be explained by considering the difference between the capillary pressure and the water hammer pressure.<sup>7,20</sup> The critical pressure that prevents the collapse of the Cassie state is the capillary pressure  $P_c$  generated by the surface textures, expressed as:  $P_c = (4\gamma \cos \theta_a)/(a-a/f)$ , where  $\theta_a$  is the advancing CA on the flat surface. According to Deng *et al.*<sup>7</sup> and Kwon *et al.*,<sup>20</sup> the transition to the Wenzel state for droplet impacting on a textured surface is attributed to the effective water hammer pressure  $P_{EWH} = k\rho VC$ , where  $\rho$  is the density of water,  $C$  is the speed of sound in water, and  $k$  is a fitting parameter that is determined by experimental condition. By balancing the hammer pressure and capillary pressure, we got the critical impact velocity. It is expected that at a velocity lower than the critical impact velocity, the capillary pressure is dominant and the droplet can exhibit a complete rebounding. Figure 3 shows the critical impact velocities for individual uniform textured samples. Shown together are the experimental data (open circles) and a theoretical curve of the critical impact velocity predicted by the capillary pres-

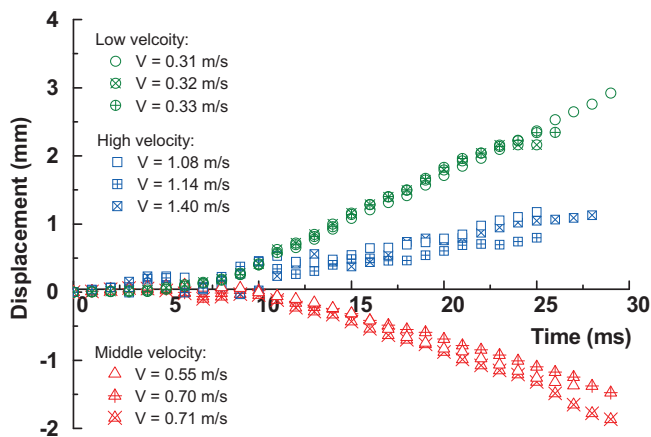


FIG. 4. (Color online) Droplet displacements on the gradient surface at different impact velocities. At low and high velocities, the droplet moves in the direction of the wettability gradient (positive values) while at intermediate velocities, the droplet moves in the direction opposite to the wettability gradient (negative values).

sure and the effective water hammer pressure with a fitting parameter  $k=0.0013$ . At an impacting velocity of 0.32 m/s, the effective water hammer pressure is estimated as 623 Pa, smaller than the capillary pressure at the collision area (1442 Pa and 779 Pa at S30 and S40, respectively). Thus, the droplet maintained in an energetically favored Cassie state after impact. However, at a high impacting velocity of 1.14 m/s, the effective water hammer pressure is 2219 Pa, much larger than the capillary pressure of S30 and S40. As a result, water droplet completely wetted the impact location covering from S20 to S50. However, at  $V=0.55$  m/s, the water droplet can only stay in the Cassie state on the large  $f$  sections (e.g., the critical velocities are 1.2 m/s and 0.75 m/s for S20 and S30, respectively) while transition to the Wenzel state took place on the small  $f$  sections (e.g., the critical velocities are 0.40 m/s and 0.30 m/s for S40 and S50, respectively). As a result, the droplet migrated in the direction where the surface has been wetted.

Figure 4 shows the lateral displacement of the droplet versus time under different impact velocities. The displacement is positive to the left and negative to the right. In the low velocity range (e.g.,  $V \sim 0.3$  m/s), no obvious displacement was observed during the spreading of the droplet (0–5 ms). In the retraction process from 5 to 10 ms, the droplet experienced a period of acceleration, during which there existed an unbalanced surface force in the lateral direction. The acceleration became less significant after 10 ms, as indicated by the relative linear slope of the displacement. The final lateral velocity reached 0.12 m/s. In the high velocity range (e.g.,  $V \sim 1.1$  m/s), when the surface was completely wetted, the unbalanced surface forces on the droplet that stays in the sticking Wenzel state was much smaller than that in the Cassie state. As a result, the lateral

velocity of the droplet was three times smaller than that in the low impact velocity cases. In the intermediate velocity range (e.g.,  $V \sim 0.6$  m/s), the centroid of the droplet fluctuated during the spreading process (0–7 ms), and then accelerated in the direction that was opposite to the wettability gradient. The maximum displacement in the intermediate velocity range was 1.6 mm, which was smaller than 2.5 mm in the low velocity range.

To summarize, we systematically investigated droplet impacting dynamics on a nonuniform superhydrophobic surface with a wettability gradient. Different from previous reports that the droplet moves toward the direction of decreasing CA, interestingly, we found that the droplet can fashion strikingly different self-migration patterns (toward or against the wettability gradient) depending on the competition of the capillary pressure and the effective water hammer pressure. Our findings highlight the importance of controlling surface roughness (wettability) and impact condition in precise manipulation of droplet placement and trajectory in microfluidics, heat transfer, and water harvesting systems.

The authors thank the Nanoelectronics Fabrication Facility at HKUST for their technical support. This work was supported by the Hong Kong RGC General Research Fund (Grant No. 621110) to S.Y. and the New Staff Startup Grant in City University of Hong Kong (7200177) to Z.W.

- <sup>1</sup>A. L. Yarin, *Annu. Rev. Fluid Mech.* **38**, 159 (2006).
- <sup>2</sup>D. Quéré, *Annu. Rev. Mater. Res.* **38**, 71 (2008).
- <sup>3</sup>Z. Wang, C. Lopez, A. Hirska, and N. Koratkar, *Appl. Phys. Lett.* **91**, 023105 (2007).
- <sup>4</sup>Y. C. Jung and B. Bhushan, *Langmuir* **24**, 6262 (2008).
- <sup>5</sup>V. Zorba, E. Stratakis, M. Barberoglou, E. Spanakis, P. Tzanetakis, S. H. Anastasiadis, and C. Fotakis, *Adv. Mater. (Weinheim, Ger.)* **20**, 4049 (2008).
- <sup>6</sup>P. C. Tsai, S. Pacheco, C. Pirat, L. Lefferts, and D. Lohse, *Langmuir* **25**, 12293 (2009).
- <sup>7</sup>T. Deng, K. K. Varanasi, M. Hsu, N. Bhate, C. Keimel, J. Stein, and M. Blohm, *Appl. Phys. Lett.* **94**, 133109 (2009).
- <sup>8</sup>M. Nosonovsky and B. Bhushan, *J. Phys.: Condens. Matter* **20**, 395005 (2008).
- <sup>9</sup>B. A. Malouin, N. A. Koratkar, A. H. Hirska, and Z. K. Wang, *Appl. Phys. Lett.* **96**, 234103 (2010).
- <sup>10</sup>M. Reyssat, F. Pardo, and D. Quéré, *EPL* **87**, 36003 (2009).
- <sup>11</sup>V. Vaikuntanathan, R. Kannan, and D. Sivakumar, *Colloids Surf., A* **369**, 65 (2010).
- <sup>12</sup>A. Shastri, M. J. Case, and K. F. Bohringer, *Langmuir* **22**, 6161 (2006).
- <sup>13</sup>G. P. Fang, W. Li, X. F. Wang, and G. J. Qiao, *Langmuir* **24**, 11651 (2008).
- <sup>14</sup>See supplementary material at <http://dx.doi.org/10.1063/1.3592997> for the static wetting properties of individual samples.
- <sup>15</sup>A. B. D. Cassie and S. Baxter, *Trans. Faraday Soc.* **40**, 546 (1944).
- <sup>16</sup>K. Y. Yeh, L. J. Chen, and J. Y. Chang, *Langmuir* **24**, 245 (2008).
- <sup>17</sup>C. Dorrier and J. Ruhe, *Langmuir* **22**, 7652 (2006).
- <sup>18</sup>J. C. Chen, *ASME J. Heat Transfer* **125**, 549 (2003).
- <sup>19</sup>R. N. Wenzel, *Ind. Eng. Chem.* **28**, 988 (1936).
- <sup>20</sup>H. Kwon, A. T. Paxson, K. K. Varanasi, and N. A. Patankar, *Phys. Rev. Lett.* **106**, 036102 (2011).